

**\*\*FULL TITLE\*\***  
*ASP Conference Series, Vol. \*\*VOLUME\*\*, \*\*YEAR OF PUBLICATION\*\**  
**\*\*NAMES OF EDITORS\*\***

## Properties of the Scattering Screen in Front of Scintillating Quasar PKS 1257-326

H. E. Bignall

*Joint Institute for VLBI in Europe, Postbus 2, 7990AA Dwingeloo, The Netherlands*

D. L. Jauncey, J. E. J. Lovell, A. K. Tzioumis

*Australia Telescope National Facility, CSIRO, PO Box 76, Epping, NSW 1710, Australia*

J.-P. Macquart

*Jansky Fellow at NRAO/Caltech. Department of Astronomy, Mail Code 105-24 Robinson, Caltech, Pasadena CA 91125, USA*

L. Kedziora-Chudczer

*Institute of Astronomy, School of Physics A28, The University of Sydney, NSW 2006, Australia*

**Abstract.** PKS 1257–326 is a quasar showing extremely unusual, rapid interstellar scintillation (ISS), which has persisted for at least a decade. Simultaneous observations with the VLA and ATCA, combined with ATCA monitoring over several years, have revealed some properties of the turbulent ionized medium responsible for the ISS of PKS 1257–326. The scattering occurs in an unusually nearby ( $\sim 10$  pc), localized “screen”. The scintillation pattern is highly anisotropic with axial ratio more than 10 : 1 elongated in a northwest direction on the sky. Recent findings and implications for small-scale ionized structures in the ISM are discussed.

### 1. Introduction

Interstellar scintillation (ISS) of compact radio sources probes structure in the ionized interstellar medium of our Galaxy down to extremely small scales ( $\sim 10^5$  km). PKS 1257–326 (Galactic coordinates  $l = 305.2^\circ$ ,  $b = 29.9^\circ$ ) is a flat spectrum, radio-loud quasar at  $z = 1.256$  which exhibits intrahour flux density variability at frequencies of several GHz due to ISS (Bignall et al. 2003). It was the third confirmed “intrahour variable” (IHV) quasar, after PKS 0405–385 (Kedziora-Chudczer et al. 1997) and J1819+3845 (Dennett-Thorpe & de Bruyn 2000).

The recent large-scale *MicroArcsecond Scintillation-Induced Variability* (MA-SIV) VLA Survey at 5 GHz showed that while a large fraction of flat-spectrum radio sources exhibit variations of typically a few percent on timescales of order a day, the IHV phenomenon is extremely rare (Lovell et al. 2003, and these proceedings). Only a handful of quasars are known to show large variations on

timescales of a few hours or less. While a source must be compact in order to scintillate, short scintillation time-scales have been attributed to nearby scattering screens within a few tens of parsec from the Sun (Dennett-Thorpe & de Bruyn 2000; Rickett et al. 2002).

## 2. Observations and analysis

We began monitoring PKS 1257–326 with the ATCA at 4.8 and 8.6 GHz in 2000 following the discovery of rapid variability (Bignall et al. 2003). We found an annual cycle in the timescale of variability which is evidently consistent over several years of observations at both frequencies. The annual cycle results from the change in scintillation velocity due to the Earth’s orbital motion. Furthermore, simultaneous observations of PKS 1257–326 with the VLA and ATCA revealed large delays of up to 8 minutes between the variability pattern arrival times at each telescope (Bignall et al. 2006), as shown in Figure 1. The two-station time delays were measured in three separate epochs, simultaneously at two frequencies and on two consecutive days in each epoch. Unlike for the case of J1819+3845 observed with the VLA and WSRT (Dennett-Thorpe & de Bruyn 2002), where the projected baseline rotated through a large angle during the simultaneous observation and the time delay changed sign, for PKS 1257–326 observed with the VLA and ATCA we detect no significant change in delay over the course of an observation. The mean pattern arrival time delays for each epoch were  $483 \pm 15$  s in 2002 May,  $333 \pm 12$  s in 2003 January, and  $318 \pm 10$  s in 2003 March. The observed annual cycle and time delays not only demonstrate conclusively that the rapid, large-amplitude variability of PKS 1257–326 is entirely due to ISS, but moreover these results can be used quantitatively to determine the bulk velocity of the scattering plasma as well as the characteristic length scale of the scintillation pattern in two dimensions.

In our analysis, the scintillation pattern is assumed to be elliptical with minor axis characteristic scale length  $a_{\min}$ , and major axis  $a_{\text{maj}} = Ra_{\min}$  oriented along the vector  $\hat{\mathbf{S}} = (\cos \beta, \sin \beta)$ . The scintillation velocity is written in the form  $\mathbf{v}(T) = v_{\text{ISS}} - v_{\oplus}(T) \equiv (v_{\alpha}(T), v_{\delta}(T))$ , and varies on an annual cycle as a function of time,  $T$  (Macquart & Jauncey 2002). Here we define  $v_{\oplus}(T)$  as the velocity of the Earth with respect to the solar system barycenter. In this notation, the time delay expected between two telescopes displaced by a distance  $\mathbf{r} = (r_{\alpha}, r_{\delta})$  is (Coles & Kaufman 1978)

$$\Delta t = \frac{\mathbf{r} \cdot \mathbf{v} + (R^2 - 1)(\mathbf{r} \times \hat{\mathbf{S}})(\mathbf{v} \times \hat{\mathbf{S}})}{v^2 + (R^2 - 1)(\mathbf{v} \times \hat{\mathbf{S}})^2}, \quad (1)$$

where the dependence of  $\mathbf{v}$  on  $T$  is suppressed. The scintillation timescale is

$$t_{\text{scint}} = \frac{a_{\min}}{\sqrt{v^2 + (R^2 - 1)(\mathbf{v} \times \hat{\mathbf{S}})^2}}. \quad (2)$$

We define  $t_{\text{scint}}$  as the point where the intensity autocorrelation function decays to  $1/e$  of its maximum value.

In practice neither the annual cycle nor the time delay experiment datasets suffice to uniquely determine all five scintillation parameters,  $v_{\text{ISS},\alpha}$ ,  $v_{\text{ISS},\delta}$ ,  $\beta$ ,  $R$

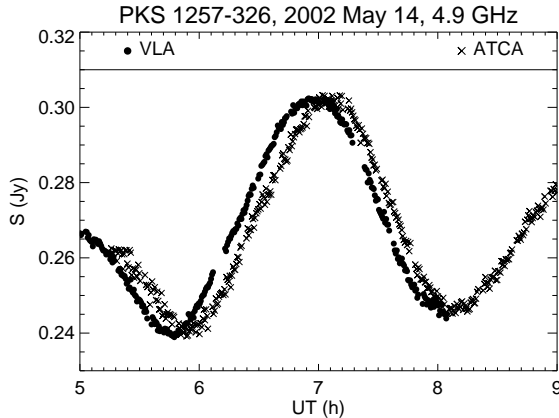


Figure 1. Simultaneous flux density measurements of PKS 1257–326 at the VLA and ATCA on 2002 May 14 at 4.9 GHz. The pattern takes 8 minutes to drift over the  $10^4$  km baseline, yet the annual cycle in timescale implies a scintillation velocity significantly larger than  $20 \text{ km s}^{-1}$  at this time of year. The large observed time delays in May are due to a highly anisotropic pattern elongated almost perpendicular to the baseline and moving with a significant velocity component parallel to the baseline.

and  $a_{\min}$ , at any one observing frequency, so we fit to both the time delay and the annual cycle data simultaneously. We also fit both frequencies simultaneously, imposing the additional constraint that the scintillation velocity is identical at the two frequencies;  $R$  and  $\beta$  at the two frequencies are still assumed independent.

## 2.1. Anisotropy

When the scintillation pattern is highly anisotropic, there are degenerate solutions for the axial ratio  $R$  and the component of velocity parallel to the major axis. However the characteristic length scale along the minor axis,  $a_{\min}$ , can still be uniquely determined. In weak scattering, as observed for PKS 1257–326 at frequencies of  $\sim 5$  GHz and above, the minor axis length scale is related to the Fresnel scale,  $r_F = \sqrt{cL/(2\pi\nu)}$ , where  $\nu$  is the observing frequency and  $L$  is the scattering screen distance. Thus  $a_{\min}$  can be used to constrain  $L$ .

For PKS 1257–326 we find that a highly anisotropic scintillation pattern is required to fit the data. The position angle of anisotropy is well constrained to within a few degrees but there is a degeneracy between the two components of the scattering screen velocity, and the pattern axial ratio  $R$  is poorly constrained. Figure 2 shows the timescale data and annual cycles from several models imposing different constraints on the parameters. For the fits shown, we weighted  $\chi^2$  to give the (comparatively few) time delay measurements equal importance in the fit relative to the characteristic timescale measurements. The dotted line in Figure 2 show that assuming an isotropic scintillation pattern results in a very poor fit to the data.

Based on the similarity of the patterns observed at the two telescopes, we can determine a lower limit for  $R$ . When the scintillation velocity has a

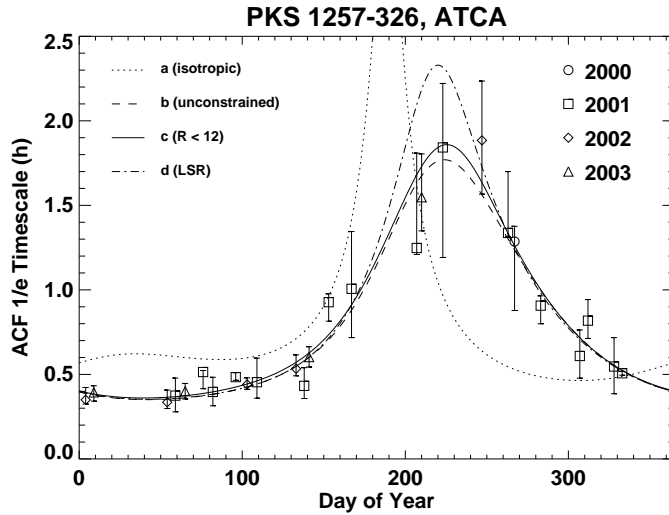


Figure 2. Annual cycle in characteristic timescale,  $t_{\text{scint}}$ , observed in ATCA data at 4.8 GHz between 2000 and 2003. The plotted lines show model annual cycles for best fits to the combined time delay and annual cycle data with (a) the scintillation pattern fixed to be isotropic ( $R = 1$ ); (b) no constraints on the parameters; (c) pattern axial ratio limited to  $R \leq 12$ ; (d) screen velocity fixed to the local standard of rest.

significant component perpendicular to the baseline  $\mathbf{r}$ , as is the case for the May time delay data, we can expect a small amount of spatial decorrelation of the scintillation pattern over the ATCA-VLA projected baseline. As detailed in Bignall et al. (2006) after careful processing of the data we can constrain the axial ratio  $R$  to be at least  $\sim 12 : 1$  based on the degree of correlation between the patterns seen at each telescope. Figure 3 shows the annual cycle in scintillation velocity for a scattering screen moving at  $-49.2 \text{ km s}^{-1}$  in RA and  $11.5 \text{ km s}^{-1}$  in Dec with respect to the Sun. The position angle of anisotropy in the scintillation pattern ( $-55^\circ$  North through East) is also illustrated by the filled ellipse in Figure 3.

As discussed by Rickett & Coles (2004, and these proceedings), there are several lines of evidence for anisotropic turbulence in the ISM. Moreover the intensity autocorrelation functions for PKS 1257–326 display strong oscillatory behaviour which is a signature of anisotropic scattering (Rickett et al. 2002). Therefore it seems likely that the large anisotropy in the scintillation pattern results from anisotropic scattering rather than anisotropic source structure. Highly anisotropic scattering suggests a plasma controlled by a magnetic field and localized in a relatively thin “screen”.

## 2.2. Distance to the scattering screen

Our best fit models give  $a_{\text{min}} = 4.24 \pm 0.08 \times 10^4 \text{ km}$  at 5 GHz, and  $a_{\text{min}} = 3.43 \pm 0.06 \times 10^4 \text{ km}$  at 8.6 GHz. For anisotropic scattering, our analysis shows that our definition of  $a_{\text{min}}$  corresponds to  $0.78r_{\text{F}}$  for a point source in weak scattering. If the source angular size is larger than the angular Fresnel scale

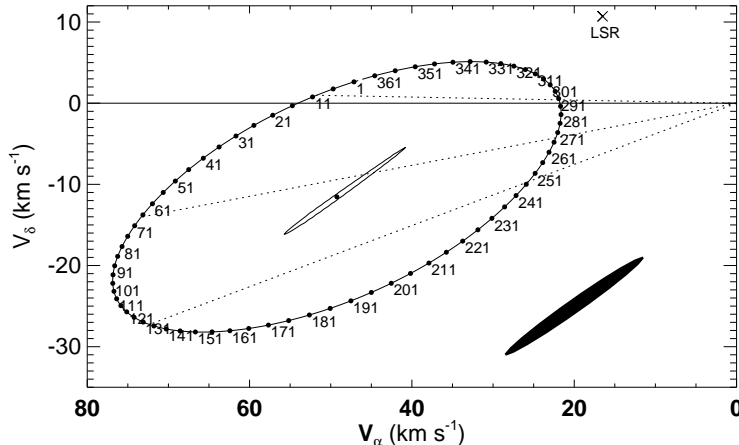


Figure 3. Scintillation velocity projected onto the plane of the sky. The large ellipse shows the annual variation of the Earth’s velocity with respect to a scattering screen moving at  $-49.2 \text{ km s}^{-1}$  in RA and  $11.5 \text{ km s}^{-1}$  in Dec with respect to the Sun, corresponding to solution (c) in Figure 2. Dotted lines indicate the velocities on the days of the time delay observations. The  $1\text{-}\sigma$  contour of the best fit solution for  $v_{\text{ISS},\alpha}$  versus  $v_{\text{ISS},\delta}$  is plotted around the best fit screen velocity at the center of the large ellipse. The component of velocity parallel to the long axis of the scintillation pattern is poorly constrained. If the scattering screen were moving with the local standard of rest, the large ellipse would be centered at position  $\times$  marked in the top right-hand corner. The black filled ellipse represents the anisotropy (position angle and axial ratio) of the best fit scintillation pattern at 4.9 GHz.

then  $a_{\text{min}}$  will be larger than  $r_{\text{F}}$ . Thus our data put an upper limit on the screen distance of  $L \lesssim 10 \text{ pc}$ .

### 2.3. The influence of source structure?

Although there is evidence for the scattering medium being largely responsible for the high degree of anisotropy in the scintillation pattern of PKS 1257–326, it is possible that source structure also plays a role in the observed scintillation.

If the scintillating component is circularly symmetric, then assuming a screen distance of 10 pc, approximately 100 mJy would have to be contained within an angular size of  $\sim 30 \mu\text{as}$  in order to display the observed large modulations. This implies a brightness temperature of at least  $T_b \sim 10^{13} \text{ K}$ , requiring a Doppler factor of 10–20 to reduce the intrinsic brightness temperature below the inverse Compton limit. Alternatively, if the “core” happened to be elongated, or consist of several components aligned in the same direction as the ISM anisotropy, then this would reduce the brightness temperature requirements. While an alignment of source structure with ISM anisotropy seems an unlikely coincidence, it is conceivable that this could be another “selection effect” for IHV. Both VLA (Bignall et al. 2006) and VLBA (Algaba, Bignall, & Reynolds 2006, in press) images of the source show broad “jet” components extended to the northwest of the core. Speculatively, if the unresolved VLBI core consists of several components on sub-mas scales also aligned in this direction, then this implies an approximate alignment of the jet with the major axis of anisotropy

in the scintillation pattern. In this case, since there is effectively only significant scattering in the direction perpendicular to the jet, the scattering screen would not “resolve” structure along the jet axis.

### 3. Conclusions

Simultaneous observations with the VLA and ATCA, combined with ATCA monitoring over several years, have revealed some properties of the scattering plasma responsible for the rapid, intrahour-timescale scintillation of PKS 1257–326. The scattering occurs in an unusually nearby ( $\sim 10$  pc), localized “screen”. Based on the longevity of the scintillation we can derive a lower limit of  $10^{15}$  cm on the linear extent of the screen. Intrahour variability is extremely rare, suggesting that these nearby screens cover a tiny fraction of the sky. The turbulence is highly anisotropic, producing a scintillation pattern with axial ratio more than 10 : 1, elongated in a northwest direction on the sky. It was suggested by J. Linksy (private communication, this conference) that the scattering could possibly be produced in turbulent regions of interaction at the edges of local clouds. It will be important to investigate the possible ISM structures responsible for the rapid scintillation of some quasars, not only to better understand the tiny-scale structure in the ionized ISM, but also to gauge the effects of ISS on observations with future sensitive cm-wavelength telescopes.

**Acknowledgments.** The ATCA is part of the Australia Telescope, which is funded by the Commonwealth of Australia for operation as a National Facility managed by CSIRO. The National Radio Astronomy Observatory is a facility of the National Science Foundation operated under cooperative agreement by Associated Universities, Inc.

### References

- Algaba, J. C., Bignall, H. E., & Reynolds, C. 2006, to appear in proceedings of Primer Encuentro de la Radioastronomía Española, May 9–11 2006, Valencia, Spain, ed. J. C. Guirado, I. Martí-Vidal, & J. M. Marcaide
- Bignall, H. E., Jauncey, D. L., Lovell, J. E. J., Tzioumis, A. K., Kedziora-Chudczer, L., Macquart, J.-P., Tingay, S. J., Rayner, D. P., & Clay, R. W. 2003, *ApJ*, 585, 653
- Bignall, H. E., Macquart, J.-P., Jauncey, D. L., Lovell, J. E. J., Tzioumis, A. K., & Kedziora-Chudczer, L. 2006, to appear in *ApJ*, 652. astro-ph/0608619
- Coles, W. A., & Kaufman, J. J. 1978, *Radio Science*, 13, 591
- Dennett-Thorpe, J., & de Bruyn, A. G. 2000, *ApJ*, 529, L65
- . 2002, *Nat*, 415, 57
- Kedziora-Chudczer, L., Jauncey, D. L., Wieringa, M. H., Walker, M. A., Nicolson, G. D., Reynolds, J. E., & Tzioumis, A. K. 1997, *ApJ*, 490, L9
- Lovell, J. E. J., Jauncey, D. L., Bignall, H. E., Kedziora-Chudczer, L., Macquart, J.-P., Rickett, B. J., & Tzioumis, A. K. 2003, *AJ*, 126, 1699
- Macquart, J.-P., & Jauncey, D. L. 2002, *ApJ*, 572, 786
- Rickett, B. J., & Coles, W. A. 2004, *Bulletin of the American Astronomical Society*, 36, 1539
- Rickett, B. J., Kedziora-Chudczer, L., & Jauncey, D. L. 2002, *ApJ*, 581, 103